

# Phase-separated states in high-pressure $\text{LaMn}_{1-x}\text{Ga}_x\text{O}_3$ manganites

M. Baldini,<sup>1</sup> D. Di Castro,<sup>1,2</sup> M. Cestelli-Guidi,<sup>3</sup> J. Garcia,<sup>4</sup> and P. Postorino<sup>1</sup>

<sup>1</sup>*Dipartimento di Fisica and CNR–INFN–Coherentia, Università di Roma “Sapienza,” Piazzale Aldo Moro 2, I-00185 Roma, Italy*

<sup>2</sup>*Dipartimento di Ingegneria Meccanica and CNR–INFN–Coherentia, Università di Roma Tor Vergata, Via del Politecnico 1, I-00133 Roma, Italy*

<sup>3</sup>*Laboratori Nazionali di Frascati–INFN, Via E. Fermi 40, 00044 Frascati, Italy*

<sup>4</sup>*Departamento de Física de la Materia Condensada, Instituto de Ciencia de Materiales de Aragon, CSIC–Universidad de Zaragoza, Pedro Cerbuna 12, 50009 Zaragoza, Spain*

(Received 30 June 2009; published 27 July 2009)

High-pressure (P) Raman ( $0 \leq P \leq 12$  GPa) and Infrared ( $0 \leq P \leq 24$  GPa) spectra are collected on two samples of the  $\text{LaMn}_{1-x}\text{Ga}_x\text{O}_3$  series:  $x=0.2$  and  $0.6$  with cooperative Jahn-Teller distorted and regular  $\text{MnO}_6$  octahedra, respectively. Raman spectra are also collected at  $P=0$  on varying Ga-content ( $0 \leq x \leq 0.8$ ). A remarkable octahedral symmetrization is observed on increasing P in the  $x=0.2$  sample, as well as  $x$  at  $P=0$ . The  $x$ -driven symmetrization process is homogeneous whereas, compressing the lattice, a phase-separated regime (regular/distorted  $\text{MnO}_6$ ) is observed at intermediate P. The comparison between the spectra of the two samples in the high-pressure regime strongly suggests the presence of small residual distortion in the  $x=0.2$  even at the highest P. Infrared data show that P is effective only in the  $x=0.2$  sample (P-driven band-gap filling) suggesting the relevance of orbital and magnetic order on the metallization process. Our results provide a unique experimental base to clarify the origin of the peculiar pressure behavior of the parent  $\text{LaMnO}_3$ .

DOI: [10.1103/PhysRevB.80.045123](https://doi.org/10.1103/PhysRevB.80.045123)

PACS number(s): 75.47.Lx, 62.50.-p, 71.30.+h, 78.30.-j

## I. INTRODUCTION

In recent years large effort was devoted to study  $\text{La}_{1-x}\text{A}_x\text{MnO}_3$  (A is a divalent metal) manganites owing to their unique and intriguing magnetotransport properties and to the promise for technological applications.<sup>1</sup> The La/A chemical substitution induces a mixed valence of the Mn ions ( $\text{Mn}^{+3}$  and  $\text{Mn}^{+4}$ ) and gives rise to dramatic changes in the physical properties of these compounds, with a variety of phases characterized by different magnetic, transport, charge, and orbital ordering properties. Hole-doped manganites ( $x \leq 0.5$ ) are commonly described in the framework of the competition between double-exchange (DE) mechanism<sup>3</sup> and localizing charge-lattice coupling triggered by the Jahn-Teller (JT) distortion of the  $\text{Mn}^{+3}\text{O}_6$  octahedra,<sup>2</sup> which allows lifting the degeneracy of the  $e_g$  levels. The  $Pbnm$  orthorhombic structure ( $O'$  type) of parent insulating  $\text{LaMnO}_3$  is characterized by strong cooperative JT distortion ( $\text{Mn}^{+3}$  ions only) and consists of a network of tilted corner-sharing  $\text{MnO}_6$  octahedra with alternate short and long Mn-O bonds in the  $ab$  plane. The onset of orbital ordered states, connected with the onset of the cooperative JT distortion, appears to notably partake in stabilizing the A-type antiferromagnetic ground state.<sup>4</sup>

Although the above picture appears rather well established, fundamental questions on interplay and relative strength of electron-lattice and electron-electron interactions in  $\text{LaMnO}_3$  are still pending.<sup>5–9</sup> In particular, a pressure (P)-induced insulator to metal transition (IMT) in  $\text{LaMnO}_3$  was observed<sup>10</sup> and afterwards theoretically investigated.<sup>6–8</sup> On applying pressure, Raman and x-ray diffraction data<sup>10</sup> show a continuous reduction in the JT distortion that appears completely suppressed above  $\sim 18$  GPa. P-symmetrized  $\text{LaMnO}_3$  surprisingly retains the insulating state up to 32 GPa, where optical reflectivity and electrical resistance mea-

surements show the system undergoes the IMT.<sup>10</sup> From this scenario, rather controversial conclusions were drawn, suggesting, for example, that the IMT is a Mott-Hubbard transition<sup>10</sup> or that, on the contrary, it is not and instead it is driven by orbital splitting of the  $e_g$  bands.<sup>6</sup> The problem is made complex even more by recent high-pressure (HP) x-ray absorption data<sup>11</sup> and theoretical results,<sup>8</sup> which call the disappearance of JT distortions at 18 GPa into question claiming their persistence up to about the IMT pressure (32 GPa).

Recent investigations on  $\text{LaMn}_{1-x}\text{Ga}_x\text{O}_3$  compounds isovalent to  $\text{LaMnO}_3$  raised further questions. The replacement of  $\text{Mn}^{3+}$  by nonmagnetic and non-JT  $\text{Ga}^{3+}$  ions remarkably reduces the cooperative JT distortion leading to a complete symmetrization of the  $\text{MnO}_6$  octahedra for  $x \geq 0.6$ .<sup>12–14</sup> A transition from the orbitally ordered  $O'$  phase ( $x \leq 0.5$ ) to the orbitally disordered O phase ( $x \geq 0.6$ ) within the  $Pbnm$  orthorhombic structure occurs simultaneously. The cooperative JT-distortion quenching also induces a reduction in the octahedra tilting angle, which diminishes on increasing Ga up to  $x=0.6$ , and keeps almost constant for  $x \geq 0.6$ . Moreover, Ga content continuously reduces the Neel temperature and an insulating FM ground state is observed for  $0.4 < x \leq 0.6$ .<sup>12</sup> As in single-valent  $\text{LaMn}_{1-x}\text{Ga}_x\text{O}_3$  the DE mechanism cannot be invoked, the last finding is explained within the framework of an orbital-flipping model, where the Ga-induced suppression of the cooperative JT distortion affects the orbital order and favors the onset of FM ordering.<sup>15</sup> Along the same line a recent thorough analysis<sup>16</sup> indicates the origin of the FM order in the orbital-mixing induced by structural bias. First HP magnetic and structural measurements on Ga-doped compounds show a breakdown of magnetic order ( $x=0$  and  $0.5$ ) and structural transitions to more symmetric phases driven by a reduction in the cooperative JT distortion on applying P.<sup>17,18</sup> The  $x$  dependence in  $\text{LaMn}_{1-x}\text{Ga}_x\text{O}_3$  thus shows a symmetrization process alternative to pressure which also allows to tune magnetic coupling

and orbital degree of freedom, with  $\text{LaMnO}_3$  lattice symmetry and volume left unchanged (the ionic radii of  $\text{Mn}^{3+}$  and  $\text{Ga}^{3+}$  are very close).

In the present paper, we aim at finding new arguments to settle the controversy on  $\text{LaMnO}_3$  pressure behavior. We are going to compare the symmetrization processes obtained by Ga substitution in  $\text{LaMn}_{1-x}\text{Ga}_x\text{O}_3$  ( $0 \leq x \leq 0.8$ ) series, which leads to a complete suppression of the JT distortion whether it is cooperative or dynamic, with that one induced by pressure ( $0 \leq P \leq 12$  GPa) in the  $\text{LaMn}_{0.8}\text{Ga}_{0.2}\text{O}_3$  (LMG20) compound which is not only isostructural to  $\text{LaMnO}_3$  (orthorhombic  $Pbnm$   $O'$  type) but presents cooperative JT distortion and orbital order. Raman spectroscopy was applied as a sensitive probe to monitor the extent of JT distortion.<sup>10,19,20</sup> The P dependence of the Raman spectrum of orbitally disordered  $\text{LaMn}_{0.4}\text{Ga}_{0.6}\text{O}_3$  (LMG60) was also investigated. Indeed, its peculiar orthorhombic O type crystalline structure characterized by regular octahedra makes it the ideal reference sample to compare with the strongly cooperative JT distorted LMG20 in order to establish if pressure is able to remove completely the octahedra distortion. Infrared (IR) spectroscopy was also applied to follow charge-delocalization processes<sup>10,21–23</sup> in LMG20 and LMG60 over a wide P range (0–24 GPa).

## II. EXPERIMENTAL PROCEDURE

Polycrystalline samples of  $\text{LaMn}_{1-x}\text{Ga}_x\text{O}_3$  manganite were prepared at high temperature by solid-state reaction: stoichiometric amounts of  $\text{La}_2\text{O}_3$ ,  $\text{MnCO}_3$ , and  $\text{Ga}_2\text{O}_3$  were mixed, milled, and fired at 1250 °C for 24 h in air. These samples were oxygen stoichiometric, within the accuracy analysis ( $\pm 0.02$ ).<sup>12</sup> Diamond-anvil cells (DAC) equipped with IIA diamonds and steel gaskets were used to apply pressure. A membrane DAC was used for Raman, whereas a small screw-clamped DAC, suitable for short working distance casegrain objective, was used for IR measurements. We adopted standard loading procedures (see Ref. 19 for Raman and Ref. 21 for IR) and the ruby fluorescence technique for *in situ* pressure measurements. Raman spectra were collected within 200–1100  $\text{cm}^{-1}$  in back-scattering geometry, using a confocal micro-Raman spectrometer (Infinity by Jobin Yvon) equipped with a 25 mW He-Ne Laser (632.8 nm), a charge-coupled device detector, and a notch filter to reject elastically scattered light. For HP Raman measurements, sample fragments (typically 200  $\mu\text{m}$  across) were selected. Raman spectra, collected from different sample points to account for possible pressure gradients,<sup>20</sup> were analyzed using a standard fitting procedure.<sup>19</sup>

## III. RESULTS AND DISCUSSION

Raman spectra at  $P=0$  of  $\text{LaMn}_{1-x}\text{Ga}_x\text{O}_3$  at different  $x$  are shown in Fig. 1. As in most of the manganitelike systems the Raman spectrum is basically dominated by the  $\text{MnO}_6$  octahedral vibrational modes.<sup>19,20</sup> The spectrum of  $\text{LaMnO}_3$  does agree with those reported in literature<sup>10,24,25</sup> and, accordingly, the main spectral structures around 500 and 600  $\text{cm}^{-1}$  are ascribed to bending (B) and *symmetric* stretching (SS)  $\text{MnO}_6$

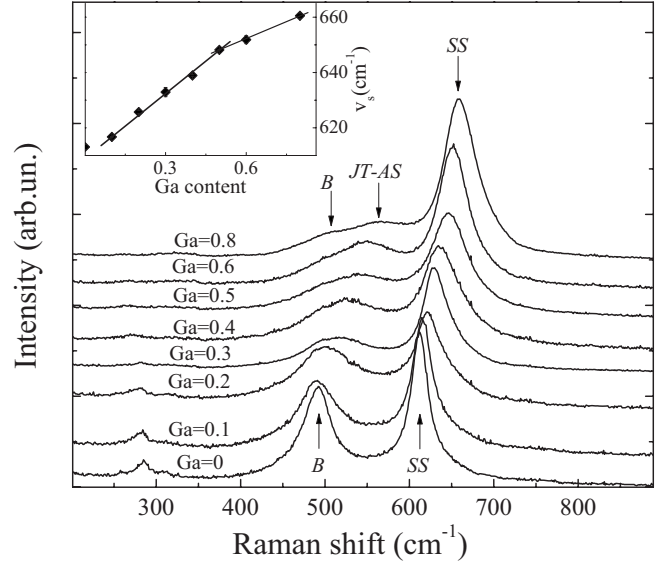


FIG. 1. Raman spectra of  $\text{LaMn}_{1-x}\text{Ga}_x\text{O}_3$ . Inset:  $x$  dependence of the symmetric-stretching frequency.

octahedral modes, respectively. The phonon peak of JT-active *antisymmetric* stretching (AS) mode at  $\sim 500$   $\text{cm}^{-1}$  previously observed by polarization analysis,<sup>25,26</sup> is apparently masked by the broad bending band centered at almost the same frequency. On increasing  $x$ , a remarkable hardening of the frequency of the SS mode is observed (faster in the  $0 < x < 0.5$  range, see inset of Fig. 1) together with the disappearance of the weak peak at about  $\sim 270$   $\text{cm}^{-1}$  for  $x > 0.5$ . These findings are related to the  $O' \rightarrow O$  structural transition since the rapid increase in the SS frequency is a marker of the JT-distortion quenching<sup>10,19,20</sup> and the low-frequency dynamic is related to the  $\text{MnO}_6$  tilting angle.<sup>25</sup> The broad two-peaks structure shown by the fully symmetric compounds ( $x=0.6$  and  $0.8$ ) can be ascribed to a B component still at  $\sim 500$   $\text{cm}^{-1}$  and to the AS mode which is expected to move at higher frequencies due to the suppression of the JT distortion ( $\sim 550$   $\text{cm}^{-1}$  see Fig. 1) and to shift faster since the sensitivity to octahedral symmetrization is much stronger for the stretching (AS and SS) than for the bending modes B.

Raman spectra of LMG20 and LMG60 at different P are shown in Fig. 2. On applying pressure, the LMG60 spectrum [Fig. 2(b)] exhibits an overall hardening of the phonon frequencies, and the two-peaks structure at  $\sim 500$   $\text{cm}^{-1}$  gets more clearly resolved owing to the strong P dependence of the stretching modes.<sup>19,20</sup>

As to LMG20 [see Fig. 2(a)], at  $\sim 2$  GPa the SS band splits into two peaks at low and high frequency (LFS at  $\sim 630$   $\text{cm}^{-1}$  and HFS at  $\sim 670$   $\text{cm}^{-1}$ ). These peaks show a strong P-driven frequency hardening and a remarkable transfer of spectral weight from LFS to HFS up to about 8 GPa, when the HFS only is observed (see Fig. 3). The comparison between the Raman spectra of LMG60 and LMG20 is shown in Fig. 3 at different pressures. At  $P=0$  the SS band of LMG20 is centered at a frequency about 50  $\text{cm}^{-1}$  lower than in LMG60. On applying P, the HFS peak appears in the LMG20 spectrum at about the same frequency as the SS

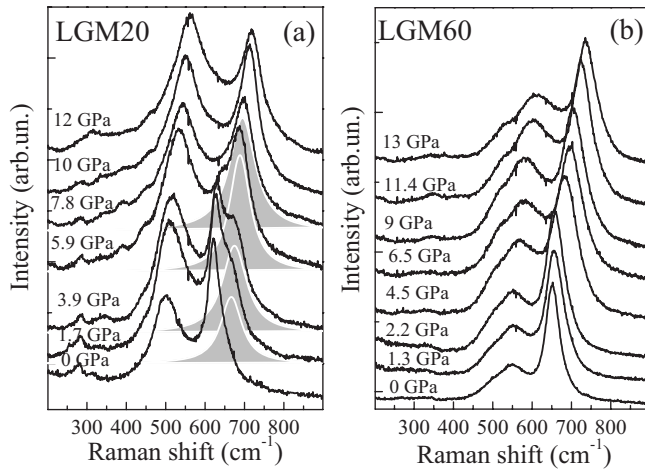


FIG. 2. Raman spectra of LGM20 and LMG60 at different pressures. Shaded areas show the HFS component as obtained from the fitting procedure.

band of LMG60 and at  $P \geq 8$  GPa, when the LFS peak disappears, the HFS and the SS peak of the LMG60 remarkably agree.

The  $P$  evolution of the Raman spectrum of LGM20, i.e., the appearance of LFS and HFS peaks at  $\sim 2$  GPa and the pressure-induced spectral weight transfer which ends up at  $\sim 8$  GPa, closely resemble the case of  $\text{LaMnO}_3$  as it is expected considering the analogies between the two samples, although the whole process occurs at different pressures. In  $\text{LaMnO}_3$ , indeed, the HFS peak appears at  $\sim 8$  GPa and the spectral weight transfer process ends up at  $\sim 18$  GPa.<sup>10</sup>

The comparison with the Raman spectra of LMG60, which consists of regular octahedra only, allow ascribe the LFS and HFS peaks in LGM20 to the stretching mode of cooperative JT-distorted and undistorted octahedra, respectively. The spectral transfer between the two stretching modes is thus the spectral signature of a pressure-induced

conversion of distorted octahedra into more regular ones. The onset and the completion of the symmetrization process occur also in  $\text{LaMnO}_3$  at pressures much higher than in LGM20 (8 and 18 GPa against 2 and 8 GPa) according to the different extent of the cooperative JT distortion in the two compounds at  $P=0$ .

Raman spectra shown in Figs. 1 and 2(a) reveal that the symmetrization processes induced by Ga doping and external pressure are basically different. The  $\text{Ga}^{+3}/\text{Mn}^{+3}$  substitution directly suppresses the distortion in  $\text{Ga}^{+3}$ -centered octahedra but has also the effect of progressively and continuously reducing the JT distortion, whether cooperative or dynamic, of  $\text{Mn}^{+3}$ -centered octahedra,<sup>12,13</sup> leading to a complete symmetrization for  $x > 0.5$ . On the other hand, although an effect in reducing the cooperative JT distortion of all the  $\text{Mn}^{+3}$ -centered octahedra can be also claimed on volume compression (hardening of the stretching frequencies), applying pressure mainly induces single octahedra to pass from a distorted to a more regular configuration (peak splitting and spectral weight transfer), thus progressively reducing the number of fully distorted octahedra down to zero at  $P \sim 8$  GPa. This finding depicts for LGM20 a phase-separation scenario for LGM20 over an intermediate pressure range (2–8 GPa) with the coexistence of fully distorted and more regular octahedra, which can be extended also to the analog compound the  $\text{LaMnO}_3$  within 8–18 GPa.<sup>10</sup> Moreover, differences between the two symmetrization processes appear also in the HP regime ( $P > 8$  GPa). Indeed, despite the symmetric-stretching modes of LGM20 and LMG60 are actually coincident, the Raman spectra appear quite distinct at lower frequencies, indicating slightly different arrangements of the octahedra network. These difference between the LGM20 and the truly symmetric LMG60 sample in the HP regime suggests a survival of a weak octahedral distortions in LGM20 which affect the octahedra tilting angle in good agreement with the theoretical analysis reported in Refs. 6 and 8.

To directly probe the effects of HP on the electronic properties, absorption spectra were collected at room temperature over the 0–24 GPa range on the same LGM20 and LMG60 compounds within the 750–6000  $\text{cm}^{-1}$  mid IR frequency range. The incident and transmitted radiation was focused and collected by a casegrain-based Hyperion 3000 IR microscope equipped with a mercury cadmium telluride detector. Spectra were collected using a Bruker Equinox 55 interferometer. Transmission measurements were carried out on slabs, about 5  $\mu\text{m}$  thick, located on the surface of a previously sintered salt pellet.<sup>21</sup> Sample slabs were obtained by pressing finely milled powder between the diamond anvils. The obtained optical densities  $O_d(\omega) = -\ln(I_T^D(\omega)/I_T^{\text{DAC}}(\omega))$ , with  $I_T^{\text{DAC}}(\omega)$  the transmitted intensity of the empty DAC without gasket and with the anvils in tight contact,<sup>23</sup> are shown in Fig. 4 for the two samples.

The spectra of LGM20 and LMG60 at the lowest pressures are rather similar: they show an intense phonon peak close to the low-frequency limit (600  $\text{cm}^{-1}$ ) followed by a band-edge behavior at higher frequencies. On the contrary, the  $P$  dependencies remarkably differ: LGM60 is actually  $P$  independent, whereas the  $O_d(\omega)$  on the high-frequency side

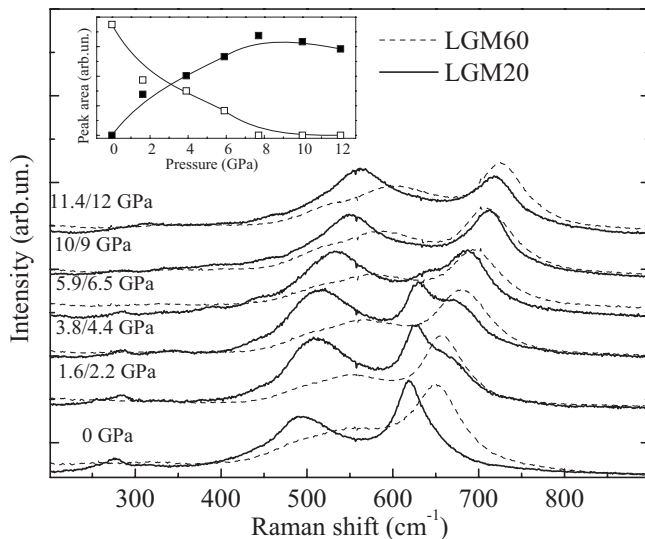


FIG. 3. Comparison between the Raman spectra of LGM20 and LMG60 under pressure. Inset: pressure dependence of the LFS and the HFS peaks intensities of LGM20.



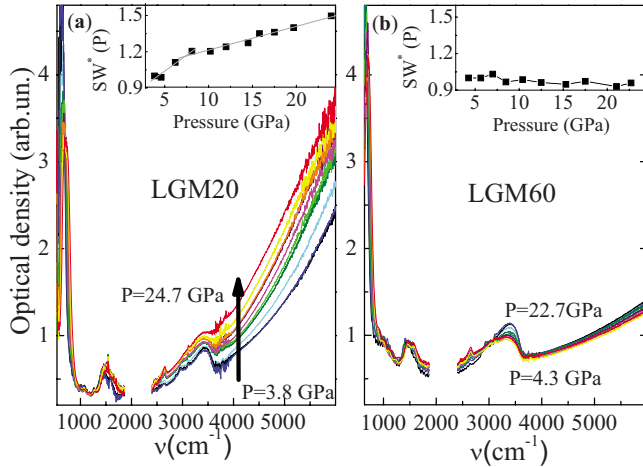


FIG. 4. (Color online) Optical densities of LGM20 and LGM60 at selected pressures. The black arrow indicates the increasing pressures. Data have been cut in the diamond absorption frequency range (around  $2000\text{ cm}^{-1}$ ). Insets: spectral weights as a function of pressure for the two samples.

of LGM20 strongly increases with pressure. The different effect on the two compounds can be better analyzed looking at the  $P$  dependence of the spectral weight  $[SW(P)]$ . At each pressure, we calculated the integral of  $O_d(\omega)$  over  $2500\text{--}4000\text{ cm}^{-1}$ , that is over the frequency range where the largest variations in the optical density are observed. The spectral weights normalized to the lowest  $P$  values  $SW^*(P) = SW(P)/SW(P_{\min})$  are shown in the insets of Fig. 4 for LGM20 and LGM60. The  $P$ -induced band-gap filling in LGM20 is rather fast within  $0 < P < 8\text{ GPa}$ , where the octahedral-symmetrization process is active, and it is still effective above  $10\text{ GPa}$ , albeit at a lower extent. This result emphasizes the role of the JT localizing tendency but clearly shows that this is not the only cause of charge localization. The quenching or, at least, the strong reduction in the octahedral distortion indeed appear to be necessary but not sufficient to enter a metallic phase, thus suggesting a non-negligible role of the electron-electron correlation.<sup>10</sup> On the other hand, the almost complete  $P$  independence of the electronic structure of LGM60 is somehow surprising since the absence of JT octahedral distortion would favor the onset of charge-delocalized states. We notice that, going from LGM20 to LGM60, the number of  $e_g$  electrons which can give rise to electrical conduction, i.e., those on the  $\text{Mn}^{3+}$  sites, is halved.

#### IV. CONCLUSION

In conclusion, Raman data clearly show that the symmetrization processes induced by Ga content and pressure in  $\text{LaMn}_{1-x}\text{Ga}_x\text{O}_3$  manganites remarkably differ. The effect of applying pressure in LGM20 is to convert  $\text{MnO}_6$  octahedra from a distorted to an undistorted (weakly distorted) configuration, passing through a phase-separated region where the coexistence of the two classes of octahedra is observed. The symmetrization process is confirmed by the coincidence of the symmetric stretching peak of LGM20 and LGM60 at HP. On the contrary, Ga substitution induces a progressive and continuous reduction in the JT distortion, whether cooperative or dynamic, leading to a complete octahedral symmetrization. The direct comparison between the  $P$ -symmetrized LGM20 with the truly symmetric LGM60 allows to point out differences in the low-frequency region of the Raman spectrum. According to theoretical literature, these differences are ascribed to the survival of distortion even when the LFS peak associated to fully distorted octahedra has disappeared. We point out that the phase-separation regime, identified in the present measurements, is a relevant point that has not been considered yet in theoretical calculations of the  $P$  behavior of  $\text{LaMnO}_3$ .<sup>6,7</sup> IR measurements on distorted LGM20 clearly link the  $P$ -induced cooperative JT-distortion reduction with the tendency toward a metallic phase. On the other hand IR and Raman results on undistorted LGM60 show that applying pressure does not affect its electronic properties and has a trivial influence on the lattice dynamics. Although the latter behavior can be ascribed to the most stable octahedral configuration, the former is more intriguing: the reduced number of potentially conductive electrons in LGM60 can indeed inhibit the onset of a metallic behavior, but bond compression and the absence of JT distortion would certainly favor a charge-delocalization process. Since pressure makes the octahedral configurations in the two compounds much closer, the origin of their peculiar  $P$  behaviors could be traced back to magnetic and orbital configurations at  $P=0$ . Present results, in addition to the previous experimental scenario,<sup>10</sup> thus provide a full set of data on  $\text{LaMnO}_3$ -like systems where the magnetic, structural, and electronic degrees of freedom, their interplay, and complex couplings are tuned, giving a unique benchmark for theoretical investigations aimed at deeper understanding of the role played by the orbital order and the magnetic interactions in these systems.

<sup>1</sup>S.-W. Cheong and H. Y. Hwang, *Colossal Magneto-Resistance Oxides*, edited by Y. Tokura, Monographs in Condensed Matter Science (Gordon and Breach, U.K., 2000) and references therein.

<sup>2</sup>A. J. Millis, *Nature (London)* **392**, 147 (1998).

<sup>3</sup>C. Zener, *Phys. Rev.* **82**, 403 (1951).

<sup>4</sup>J. B. Goodenough, *Phys. Rev.* **100**, 564 (1955).

<sup>5</sup>W.-G. Yin, D. Volja, and W. Ku, *Phys. Rev. Lett.* **96**, 116405

(2006).

<sup>6</sup>A. Yamasaki, M. Feldbacher, Y.-F. Yang, O. K. Andersen, and K. Held, *Phys. Rev. Lett.* **96**, 166401 (2006).

<sup>7</sup>G. Trimarchi and N. Binggeli, *Phys. Rev. B* **71**, 035101 (2005).

<sup>8</sup>J. D. Fuhr, M. Avignon, and B. Alascio, *Phys. Rev. Lett.* **100**, 216402 (2008).

<sup>9</sup>R. Tyer, W. M. Temmerman, Z. Szotek, G. Banach, A. Svane, L. Petit, and G. A. Gehring, *Europhys. Lett.* **65**, 519 (2004).

- <sup>10</sup>I. Loa, P. Adler, A. Grzechnik, K. Syassen, U. Schwarz, M. Hanfland, G. K. Rozenberg, P. Gorodetsky, and M. P. Pasternak, *Phys. Rev. Lett.* **87**, 125501 (2001).
- <sup>11</sup>A. Y. Ramos, H. C. N. Tolentino, N. M. Souza-Neto, J. P. Itié, L. Morales, and A. Caneiro, *Phys. Rev. B* **75**, 052103 (2007).
- <sup>12</sup>J. Blasco, J. Garcia, J. Campo, M. C. Sanchez, and G. Subias, *Phys. Rev. B* **66**, 174431 (2002).
- <sup>13</sup>M. C. Sanchez, G. Subias, J. Garcia, and J. Blasco, *Phys. Rev. B* **69**, 184415 (2004).
- <sup>14</sup>M. C. Sanchez, J. Garcia, G. Subias, and J. Blasco, *Phys. Rev. B* **73**, 094416 (2006).
- <sup>15</sup>J. Farrell and G. A. Gehring, *New J. Phys.* **6**, 168 (2004).
- <sup>16</sup>J.-S. Zhou and J. B. Goodenough, *Phys. Rev. B* **77**, 172409 (2008).
- <sup>17</sup>J.-S. Zhou, Y. Uwatoko, K. Matsubayashi, and J. B. Goodenough, *Phys. Rev. B* **78**, 220402(R) (2008).
- <sup>18</sup>M. Baldini, L. Malavasi, D. Di Castro, A. Nucara, W. Crichton, M. Mezouar, J. Blasco, and P. Postorino, arXiv:0807.2848 (unpublished).
- <sup>19</sup>A. Congeduti, P. Postorino, E. Caramagno, M. Nardone, A. Kumar, and D. D. Sarma, *Phys. Rev. Lett.* **86**, 1251 (2001).
- <sup>20</sup>P. Postorino, A. Congeduti, E. Degiorgi, J. P. Itie, and P. Munsch, *Phys. Rev. B* **65**, 224102 (2002).
- <sup>21</sup>P. Postorino, A. Congeduti, P. Dore, A. Sacchetti, F. Gorelli, L. Ulivi, A. Kumar, and D. D. Sarma, *Phys. Rev. Lett.* **91**, 175501 (2003).
- <sup>22</sup>A. Congeduti, P. Postorino, P. Dore, A. Nucara, S. Lupi, S. Merccone, P. Calvani, A. Kumar, and D. D. Sarma, *Phys. Rev. B* **63**, 184410 (2001).
- <sup>23</sup>A. Sacchetti, M. C. Guidi, E. Arcangeletti, A. Nucara, P. Calvani, M. Piccinini, A. Marcelli, and P. Postorino, *Phys. Rev. Lett.* **96**, 035503 (2006).
- <sup>24</sup>C. Aruta, M. Angeloni, G. Balestrino, N. G. Boggio, P. G. Medaglia, A. Tebano, B. Davidson, M. Baldini, D. Di Castro, P. Postorino, P. Dore, A. Sidorenko, G. Allodi, and R. De Renzi, *J. Appl. Phys.* **100**, 023910 (2006).
- <sup>25</sup>M. N. Iliev, M. V. Abrashev, H.-G. Lee, V. N. Popov, Y. Y. Sun, C. Thomsen, R. L. Meng, and C. W. Chu, *Phys. Rev. B* **57**, 2872 (1998).
- <sup>26</sup>M. N. Iliev and M. V. Abrashev, *J. Raman Spectrosc.* **32**, 805 (2001).